

Tradeoff Analysis of Delay-Power-CSIT Quality of Dynamic BackPressure Algorithm for Energy Efficient OFDM Systems

Vincent K. N. Lau and Chung Ha Koh

Dept. of Electrical and Computer Engineering

Hong Kong University of Science and Technology, Hong Kong

Email: {eeknlau, eechungha}@ust.hk

Abstract

In this paper, we analyze the fundamental power-delay tradeoff in point-to-point OFDM systems under imperfect channel state information quality and non-ideal circuit power. We consider the dynamic backpressure (DBP) algorithm, where the transmitter determines the rate and power control actions based on the instantaneous channel state information (CSIT) and the queue state information (QSI). We exploit a general fluid queue dynamics using a continuous time dynamic equation. Using the sample-path approach and renewal theory, we decompose the average delay in terms of multiple *unfinished works* along a sample path, and derive an upper bound on the average delay under the DBP power control, which is asymptotically accurate at small delay regime. We show that despite imperfect CSIT quality and non-ideal circuit power, the average power (P) of the DBP policy scales with delay (D) as $P = \mathcal{O}(D \exp(1/D))$ at small delay regime. While the impacts of CSIT quality and circuit power appears as the coefficients of the scaling law, they may be significant in some operating regimes.

⁰This work has been supported by Huawei Technologies.

I. INTRODUCTION

There is a growing awareness of energy efficiency of the wireless infrastructure. In [1], [2], the authors considered adaptive power control to optimize an energy efficiency metric, namely the Joule per bit. This metric measures the average cost (i.e. energy) to the generated utility (i.e. information bits) and allows for accessing the energy efficiency at full loads. However, this metric does not incorporate the delay aspect. Furthermore, in all these works, perfect channel state information (CSIT) is assumed and the issues of packet errors are ignored. There have been several works that consider robust power control by taking into account of the imperfect CSIT. In [3], [4], the authors derived a power adaptation algorithm to maximize the system goodput accounting for potential packet errors due to imperfect CSIT. There are also some works that consider MIMO design with imperfect CSIT [3], [5] or limited feedback [6]. While these works have dealt with the impact of imperfect CSIT, they have ignored the burstiness as well as the delay performance of the source data.

In general, it is quite challenging to consider delay optimization in wireless systems because that involves a joint consideration of both the information theory (to model the PHY dynamics) and the queueing theory (to model the delay dynamics). One general approach to delay optimal control is to use Markov Decision Process (MDP) and the optimal control is given by the Bellman equation [7]. However, it is well known that there is no simple solution to the Bellman equation and one cannot obtain viable solutions using brute force value iteration or policy iteration. Another approach is to adopt Lyapunov theory to derive the *throughput optimal* control policy¹ [9]. While the control policy derived is adaptive to both the CSIT and QSI, the delay performance of such schemes are not fully understood. In [10], the authors derived the *dynamic backpressure* (DBP) control and the well-known asymptotic power-delay tradeoff of $\mathcal{O}(1/V)$, $\mathcal{O}(V)$ as $V \rightarrow \infty$, i.e., at large delay regime². Furthermore, all these existing works have assumed perfect CSIT and it is not clear how

¹Throughput-optimal policies are the set of policies which can stabilize the queues in the system if the arrival rate vector is inside the *stability region* [8].

² V is a constant which determines the tradeoff between power consumption and delay performance. We use the following notation in [11] to characterize the asymptotic behavior a function $g(x)$ as $x \rightarrow x^*$: $g(x) = \mathcal{O}(f(x))$, if $\limsup_{x \rightarrow x^*} \frac{g(x)}{f(x)} < \infty$; $g(x) = \Omega(f(x))$, if $\limsup_{x \rightarrow x^*} \frac{f(x)}{g(x)} < \infty$; $g(x) = \Theta(f(x))$, if $g(x) = \mathcal{O}(f(x))$, and $g(x) = \Omega(f(x))$.

the CSIT quality will affect the underlying delay power tradeoff.

In this paper, we are interested to study the inter-relationship between energy efficiency, CSIT quality and delay performance of the DBP algorithm for OFDM systems. The following are some first order technical challenges that have to be overcome:

- **Coupling between the Control Policy and the Queue Dynamics:** The DBP algorithm is adaptive to both the QSI and CSIT and hence, this introduces coupling to the queue dynamics and the control actions at each frame. This coupling makes the delay analysis of the system extremely difficult because there is no closed-form expression for the steady state distribution of the queue length for such dynamic policy. While there are some works in the literature that analyze the delay-power tradeoff for DBP algorithms using Lyapunov bounds [10], such analyses are focused on the first order analysis. However, such Lyapunov bounding techniques are usually very loose and cannot be used to study the second order impacts of system parameters such as how the CSIT quality affects the delay performance.
- **Coupling of Imperfect CSIT and Energy Efficiency:** For a given delay requirement, we should reduce the transmission data rate so as to increase the transmission time [12], [13] for energy efficient communications³. However, the underlying tradeoff changes when circuit power and imperfect CSIT are taken into account. By circuit power, we refer to the power consumption in the RF transmission chain, which can be assumed to be constant irrespective of the transmission rate. Thus, it is not always energy efficient to lengthen the transmission time up to the delay limit because the energy expenditures resulting from circuit power are proportional to the transmission time. On the other hand, due to imperfect CSIT, the transmission power required to support a certain goodput depends on the CSIT quality. Yet, quantifying this relationship for OFDM systems with joint encoding across subcarriers is not trivial because that involves finding the CDF of the mutual information.
- **Performance in Small Delay Regime:** Another potential limitation of the Lyapunov bounding technique is that it works for asymptotically large delay regime, which is usually not the regime we are interested in. There are not many works on the analysis of small delay regions. In [11], the authors studied the

³This is because the transmission power increases exponentially with data rate.

delay-power tradeoff of a bounded rate scheme in fading channels at small delay regime under perfect CSIT. However, the delay performance of DBP algorithm in OFDM systems at small delay regime as well as the impact of CSIT quality are still not well-understood.

In this paper, we overcome the above challenges using continuous time stochastic calculus [14], [15]. For instance, we introduce a *virtual continuous time system* (VCTS) and model the fluid queue dynamics using a continuous time dynamic equation [13], [16]. Using a calculus approach, we first derive closed-form expressions for the *unfinished work* in between arrivals. To analyze the end-to-end average delay performance, we adopt and extend the sample-path approach [15] and decompose the average delay in terms of multiple *unfinished works* along a sample path using renewal reward theory. As such, we obtained an asymptotically accurate upper bound on the average delay under the DBP power control at small delay regime. We show that despite imperfect CSIT quality and non-ideal circuit power, the average power (P) of the DBP policy scales with delay (D) as $P = \mathcal{O}(D \exp(1/D))$ at small delay regime. While the impacts of CSIT quality and circuit power appears as the coefficients of the scaling law, they may be significant in some operating regimes.

TABLE I
NOTATION USED THROUGHOUT THE PAPER

Symbol	Meaning
Δt	time duration of a scheduling slot
T	time duration of a arrival period
\overline{B}	the average of arriving packet size
$U(k)$	total number of remaining bits at k -th scheduling slot in a queue
$\tilde{U}(t)$	fictitious queue state at continuous time t
ε	target packet error rate
n_F	the number of subcarriers
σ_e^2	the variance of the CSIT error
$\overline{j^U}$	per-period average unfinished work
$\overline{j^g}$	per-period average energy consumption
$\overline{J^U}$	continuous time per-period average unfinished work
$\overline{J^g}$	continuous time per-period average energy consumption
$\bar{d}(\Omega)$	average (end-to-end) delay of a policy Ω
$\bar{g}(\Omega)$	average power consumption of a policy Ω

II. SYSTEM MODEL

In this section, we shall elaborate the system model of the OFDM link, including the physical layer model, the bursty source model, the queueing dynamics and the power consumption model.

A. Frequency Selective Fading Channel Model and the Imperfect CSIT Model

We consider a point-to-point OFDM system with n_F subcarriers. The number of resolvable paths in the frequency selective channel is given by $N_d = \left\lfloor \frac{W}{\Delta f_c} \right\rfloor$, where W is the signal bandwidth and Δf_c is the coherence bandwidth. The channel impulse response can be described by:

$$h(t, v) = \sum_{l=1}^{N_d} h_l(t) \delta \left(v - \frac{l}{W} \right)$$

where $\frac{l}{W}$ is the time delay of the l -th path and $h_l(t)$ is the corresponding circularly symmetric complex Gaussian (CSCG) random fading coefficients with zero mean and variance σ_l^2 (σ_l^2 defines the power-delay profile). Using n_F -point IFFT and FFT in the OFDM system, the received signal in the frequency domain is given by:

$$Z_n = H_n \cdot S_n + w_n,$$

where S_n and Z_n are the transmit and receive signals, respectively, of the n -th subcarrier and w_n is the i.i.d. complex Gaussian noise with zero mean and normalized variance $1/n_F$ (so that the total noise power across the n_F subcarriers is unity). Note that $H_n = \sum_{l=1}^{N_d} h_l e^{\frac{-j2\pi ln}{n_F}}$ for all n , which is the FFT of the time-domain channel fading coefficients $\{h_0, \dots, h_{N_d-1}\}$.

For simplicity, we consider a TDD system and the transmitter obtains an estimate of the CSIT based on the reciprocal reverse channel [17]. However, due to the channel estimation noise as well as the TDD duplexing delay, the estimated CSIT may be outdated. Assume that the CSIT is estimated using MMSE prediction in the time domain, the CSIT model in the time domain is given by:

$$\hat{h}_l = h_l + \Delta h_l, \quad \Delta h_l \sim \mathcal{CN}(0, \sigma_{h,l}^2), \quad l \in \{0, 1, \dots, N_d - 1\}.$$

where $\sigma_{h,l}^2 = 1 - \frac{E_p \sigma_l^2}{E_p \sigma_l^2 + 1} J_0(2\pi f_D \tau)$, E_p is the pilot SNR, J_0 is a Bessel function of the first kind of order 0, f_D is the Doppler shift, and τ is the duplexing delay [18], [19]. Thus, the estimated CSIT in the frequency

domain \widehat{H}_n after n_F -point FFT of $\{\widehat{h}_1, \dots, \widehat{h}_{N_d-1}\}$ is as follows:

$$\widehat{H}_n = H_n + \Delta H_n \quad (1)$$

where H_n is the actual channel state information (CSI) of the n -th subcarrier and ΔH_n represents the CSIT error. The CSIT errors ΔH_n is CSCG with zero mean and variance $\sigma_n^2 = \sum_{l=1}^{N_d} \sigma_{h,l}^2$, and the correlation of the CSIT error between the n_1 -th and n_2 -th subcarriers is given by: $\mathbb{E}[\Delta H_{n_1} \Delta H_{n_2}^H] = \sum_{l=1}^{N_d} \sigma_{h,l}^2 e^{\frac{-j2\pi l(n_1 - n_2)}{n_F}}$.

We model the packet error solely by the probability that the scheduled data rate exceeds the instantaneous mutual information. Note that the packet errors due to imperfect CSIT is systematic and cannot be eliminated by simply using strong channel coding. Therefore we shall exploit diversity to protect the information from channel outage to enhance the chance of successful delivery to the receiver. Specially, the encoded symbols are transmitted over the frequency domain via a random frequency interleaver. The conditional packet error probability (PER) ε (conditioned on the CSIT $\widehat{\mathbf{H}}$ and the QSI U) of a transmission with data rate r (nat/sec) is given by: $\Pr \left[r > \sum_{n=0}^{n_F-1} \log \left(1 + \frac{P_{tx} |H_n|^2}{n_F} \right) \middle| \widehat{\mathbf{H}}, U \right]$ where P_{tx} is the transmit power. $\widehat{\mathbf{H}} \triangleq \left(\widehat{H}_0, \dots, \widehat{H}_{n_F-1} \right)^T$ indicates the estimated CSIT which is described in (1) and U denotes the queue length (in number of bits) [U is defined in Section II.B].

Remark 1 (Power Allocation over Subcarriers): In this paper, we have assumed uniform power allocation over subcarriers for the following reasons. First, there is no known closed form expression conditional cdf of mutual information $\sum_{n=0}^{n_F-1} \log \left(1 + \frac{P_{tx} |H_n|^2}{n_F} \right)$. Second, for moderate CSIT quality, the performance bottleneck is the packet errors (due to the residual uncertainty of mutual information given inaccurate CSIT). As a result the first order factor is diversity. Based on uniform power allocation, we have shown (Lemma 1) that full diversity order can be captured. Third, we have compared the performance of optimized power allocation (obtained by stochastic gradient method [20], [21]) versus uniform power allocation in Fig. 6 and it is shown that power optimization over subcarriers only shows marginal gain at moderate CSIT quality. ■

B. Bursty Source Model, Queue Dynamics and Dynamic Rate Control Policy

In this paper, we consider a bursty bit flow model. The time dimension is partitioned into scheduling slots of duration Δt and indexed by k . Multiple slots are grouped as a frame of duration T and indexed by m as

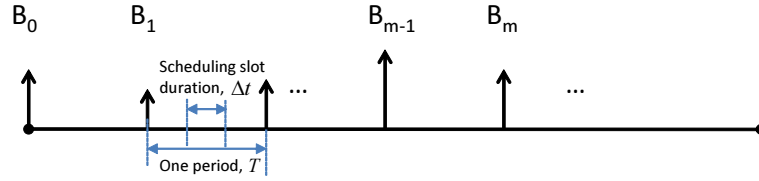


Fig. 1. The random arrival and delay deadline model.

illustrated in Fig. 1. We have the following assumptions regarding the CSI and the bursty source model.

Assumption 1 (Quasi-Static CSI): For notation convenience, we denote $\hat{\mathbf{H}}(k) \triangleq (\hat{H}_0(k), \dots, \hat{H}_{n_F-1}(k))^T$ and $\mathbf{H}(k) \triangleq (H_0(k), \dots, H_{n_F-1}(k))^T$ as the $n_F \times 1$ dimension CSIT and CSI vectors, respectively, at the k -th scheduling slot. The CSI $\mathbf{H}(k)$ is assumed to be quasi-static within a scheduling slot and i.i.d. between scheduling slots. ■

Assumption 2 (Bursty Source Model): Let \mathcal{B}_m be the random new arrivals (in bits) at the m -th frame. The arrival process $\{\mathcal{B}_m\}$ is i.i.d. over m according to a general distribution $\Pr(\mathcal{B})$ with average $\mathbb{E}[\mathcal{B}_m] = T\bar{B}$ where \bar{B} is the average arrival rate per second. ■

The QSI $U(k)$ is defined as the *unfinished work* (i.e. the total number of remaining bits) in the queue at the beginning of the k -th scheduling slot. Let $\chi(k) = (U(k), \hat{\mathbf{H}}(k))$ be the system state at the k -th scheduling slot. Given an observed system state χ , the transmitter adjusts the transmit data rate according to a stationary rate control policy defined below.

Definition 1 (Stationary Rate Control Policy): Let $r(k)$ be the rate allocation action of the OFDM transmitter at the k -th scheduling slot. A stationary rate control policy Ω is a mapping from the system state χ to a rate control action r . Specifically, $r(k) = \Omega(\chi(k))$ for all k . ■

Given a stationary rate control policy Ω , the queue dynamics is given by:

$$U(k+1) = [U(k) - r(k)(1 - e(k))\Delta t]^+ + \mathcal{B}_{\lfloor \frac{k\Delta t}{T} \rfloor} \mathbf{1}(\text{mod}(k, T/\Delta t) = 0) \quad (2)$$

where $x^+ = \max\{x, 0\}$ and $e(k) \in \{0, 1\}$ is the packet error indicator at the k -th scheduling slot⁴.

⁴We assume there is an error-free and delay-free ACK/NAK feedback from the receiver to the transmitter.

C. Power Consumption Model

At the transmitter, the power consumption is contributed by the *transmission power* of the power amplifier and the *circuit power* of the RF chains (such as the mixers, synthesizers, phase-lock loop and digital-to-analog converters). The transmission power P_{tx} in general depends on the transmitted data rate r as well as the CSIT quality. Specifically, the transmitted data rate is given by $r = n_F \log(1 + \frac{P}{n_F} f(\varepsilon, \sigma_e^2, \hat{\mathbf{H}}))$ for a target PER ε [22], where $f(\varepsilon, \sigma_e^2, \hat{\mathbf{H}})$ is a “black box function” which characterizes the behavior of the underlying PHY under imperfect CSIT. In other words, for a given data rate r , CSIT error σ_e^2 and target PER ε , the minimum required transmission power is given by

$$P_{tx}(r; \hat{\mathbf{H}}) = \frac{\left(e^{\frac{r}{n_F}} - 1\right) n_F}{f(\varepsilon, \sigma_e^2, \hat{\mathbf{H}})} \quad (3)$$

For uniform power-delay profile⁵, the following lemma summarizes an asymptotically accurate relationship at high and low SNR.

Lemma 1 (Relationship between Transmit Power and CSIT Quality): Under uniform power-delay profile, for a given data rate r , CSIT error σ_e^2 and target PER ε , $f(\varepsilon, \sigma_e^2, \hat{\mathbf{H}})$ in (3) is given by:

$$f(\varepsilon, \sigma_e^2, \hat{\mathbf{H}}) \doteq F_{\psi^2; s^2}^{-1}(\varepsilon) \quad (4)$$

where \doteq denotes asymptotic equality for high and low SNR and $F_{\psi^2; s^2}^{-1}$ is the inverse CDF of the non-central chi-square random variable ψ^2 with non-centrality parameter s^2 . The chi-square random variable $\psi^2 = \frac{1}{N_d} \sum_{n \in I_B} |H_n|^2$ has $2N_d$ degrees of freedom and variance σ_e^2/N_d , where I_B is the set of N_d independent subcarriers. The non-centrality parameter is given by $s^2(I_B) = \frac{1}{N_d} \sum_{n \in I_B} |\hat{H}_n|^2$. ■

Proof: Due to page limitation, please refer to [22] for the proof. ■

The transmission power $P_{tx}(r; \hat{\mathbf{H}})$ is a convex increasing function of the data rate r . On the other hand, the CSIT quality affects the $P_{tx}(r; \hat{\mathbf{H}})$ via the variance of the inverse chi-square CDF $F_{\psi^2; s^2}^{-1}(x)$. Specifically, a larger transmission power is required for the same data rate r when the CSIT error increases. Fig. 2 illustrates

⁵Uniform power delay profile is known to be the worst case profile in frequency selective fading channels [23], [24]. As a result, the closed form expression for $f(\varepsilon, \sigma_e^2, \hat{\mathbf{H}})$ in Lemma 1 represents the worst case profile. For general power delay profile, there is no closed form expression for $f(\varepsilon, \sigma_e^2, \hat{\mathbf{H}})$ but it can be obtained via offline PHY level simulation.

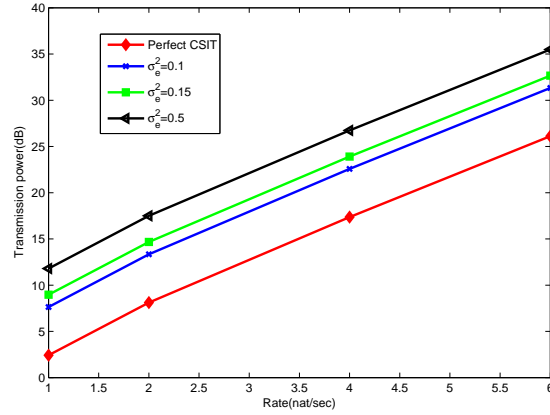


Fig. 2. Required transmission power (dB) versus data rate with different CSIT error σ_e^2 , target PER=0.01, single subcarrier, bandwidth = 1Hz.

the $P_{tx}(r; \hat{\mathbf{H}})$ versus r at different CSIT errors under uniform power-delay profile. Observe that a larger transmission power is required for the same data rate r when the CSIT error increases.

On the other hand, the circuit power P_{cct} is constant regardless of the transmission data rate. The transmission circuit is assumed to be on during the transmission of a burst. Hence, the total power consumption at the transmitter during a burst is given by:

$$g(r, \chi) = P_{tx}(r, \hat{\mathbf{H}}) + P_{cct}.$$

Note that there are two conflicting dynamics due to (a) bursty arrivals and (b) energy efficiency regarding whether one should increase the transmission time to finish the data backlog. It is known [25] that one should try to reduce the data rate when the buffer level is small so as to decrease the chance of the buffer being empty. Furthermore, the transmission power increases exponentially with the data rate and hence, one should increase the transmission time so as to save energy [13]. On the other hand, when the circuit power is taken into consideration, the tradeoff dynamics will be changed because the energy expenditures resulting from circuit power are proportional to the transmission time of the system [26]. As a result, it is not always advantageous to increase the transmission time.

III. DYNAMIC BACKPRESSURE POWER CONTROL

In this section, we first focus on a queue stabilization problem and derive the throughput optimal policy DBP using the Lyapunov function $L(U) = U^2/2$ [27].

A. Preliminaries of Stochastic Stability

We first introduce a few definitions. We say that the OFDM link with bursty arrival is *strongly stable* if:

$$\limsup_{K \rightarrow \infty} \frac{1}{K} \sum_{k=1}^K \mathbb{E}[U(k)] < \infty .$$

Definition 2 (Stability Region): The stability region Λ_Ω of policy Ω is the set of average arrival rates λ for which the system is stable under Ω . The stability region of the system Λ is the closure of the set of all average arrival rates λ for which a stabilizing control policy exists. Mathematically, we have $\Lambda = \bigcup_{\Omega \in G} \Lambda_\Omega$, where G denotes policy space. ■

Definition 3 (Throughput-Optimal Policy): A throughput-optimal policy dominates⁶ any other policy in G , i.e. it has a stability region that is the superset of the stability region of any other policy in G . Therefore, it should have a stability region equal to Λ . ■

In other words, throughput-optimal policies ensure that the queueing system is stable as long as the vector arrival rate is within the system stability region Λ . Note that the throughput optimal policy is not unique. While throughput optimality does not guarantee delay optimality in the system, the former policy can still improve the delay performance. Furthermore, using Lyapunov analysis techniques [9], the throughput optimal policy derived usually has a simple form, which is desirable for implementation.

Consider the Lyapunov function $L(U) = U^2/2$ [27], and define the one-step Lyapunov drift $\Delta L(U)$ as:

$$\Delta(L(U(k))) \triangleq \mathbb{E}[L(U(k+1)) - L(U(k)) | U(k)] . \quad (5)$$

The following Lemma summarizes the results on the Lyapunov drift.

Lemma 2 (Lyapunov Drift): Let $A(k)$ be the arrival process of queue dynamics (2). Furthermore, let $A(k) \leq A_{\max}$ and $r(k)(1 - e(k))\Delta t \leq R_{\max}$, for some positive A_{\max} and R_{\max} . The one step Lyapunov

⁶A policy Ω_1 *dominates* another policy Ω_2 if $\Lambda_{\Omega_2} \subset \Lambda_{\Omega_1}$.

drift for the OFDM link with imperfect CSIT is given by:

$$\Delta(L(U(k))) \leq \frac{1}{2}(A_{\max}^2 + R_{\max}^2) - \mathbb{E}[U(k) \{r(k)(1 - e(k))\Delta t - A(k)\} | U(k)] \quad (6)$$

Proof: The proof follows similar technique as in [9] and is omitted. ■

B. Dynamic BackPressure Algorithm

Based on the Lyapunov drift $\Delta(L(U(k)))$ in Lemma 2, the DBP algorithm can be derived by maximizing the negative drift term in (6). Given an observed state χ at any scheduling time slot, the instantaneous data rate $r_{DBP}(U, \hat{\mathbf{H}})$ is given by:

$$r_{DBP}(U, \hat{\mathbf{H}}) = \arg \max_r \left\{ Ur(1 - \varepsilon)\Delta t - V \left(P_{tx}(r; \hat{\mathbf{H}}) + P_{cct} \right) \Delta t \right\} \quad (7)$$

where V is a constant which determines the tradeoff between power consumption and delay performance.

Solving the problem in (7) for the DBP, the instantaneous data rate $r_{DBP}(\chi)$ is given by:

$$r_{DBP}(\chi) = n_F \left[\log \left\{ \frac{U(1 - \varepsilon)f(\epsilon, \sigma_e^2, \hat{\mathbf{H}})}{V} \right\} \right]^+ \quad (8)$$

During a burst transmission, the instantaneous power consumption under DBP is given by:

$$g_{DBP}(\chi) = \begin{cases} \frac{U(1-\varepsilon)n_F}{V} - \frac{n_F}{f(\epsilon, \sigma_e^2, \hat{\mathbf{H}})} + P_{cct}, & \text{if } \frac{U(1-\varepsilon)n_F}{V} - \frac{n_F}{f(\epsilon, \sigma_e^2, \hat{\mathbf{H}})} > 0 \\ 0, & \text{otherwise.} \end{cases} \quad (9)$$

Remark 2 (Multilevel Water-Filling Structure of the DBP): The power control action in (9) is a function of both CSIT and QSI (where it depends on the CSIT indirectly via the noncentrality parameter $s^2(I_B) = \frac{1}{N_d} \sum_{n \in I_B} |\hat{H}_n|^2$ in $f(\epsilon, \sigma_e^2, \hat{\mathbf{H}})$). It has the form of *multilevel water-filling structure* where the transmission power is allocated according to the CSIT but the waterlevel is adaptive to the QSI. The parameter V acts like the Lagrange Multiplier which determines the tradeoff between power consumption and delay. Furthermore, the P_{cct} affects the power control (or rate control solution) in (9) and (8) by introducing a penalty proportional to a burst transmission time. ■

IV. DELAY-POWER TRADEOFF OF DBP WITH IMPERFECT CSIT

While the DBP is throughput optimal, we are interested in studying the end-to-end delay performance and the relationship between the average delay, average power and the CSIT quality. In this section, we shall

analyze the power-delay tradeoff using continuous time approximation and renewal process theory. As we shall illustrate, this approach not only yields first order tradeoff relationship (at small delay regime) but also yields the second-order impacts due to imperfect CSIT and static circuit power P_{cct} .

A. Per-Period Unfinished Works

To analyze the average delay, we first focus on the analysis of one arrival period T . Specifically, define the per-period average unfinished work $\overline{j^U}(U_0)$ and the per-period average energy consumption $\overline{j^g}(U_0)$ as:

$$\overline{j^U}(U_0) = \mathbb{E} \left[\sum_{k=0}^{N-1} U_k \Delta t \mid U_0 \right] \quad (10)$$

$$\overline{j^g}(U_0) = \mathbb{E} \left[\sum_{k=0}^{N-1} g(r(k), \chi(k)) \Delta t \mid U_0 \right] \quad (11)$$

where U_0 is the leftover bits at the buffer at the starting epoch of a period T . To compute $\overline{j^U}(U_0)$ and $\overline{j^g}(U_0)$, we shall adopt a continuous time approach. Specifically, we define a *virtual continuous time system* (VCTS) as follows:

Definition 4 (Virtual Continuous Time Systems): A virtual continuous time system is a fictitious system with a continuous queue state $\tilde{U}(t)$ and channel state $\tilde{\mathbf{H}}(t)$. The fictitious queue state evolves according to the following dynamic equation:

$$\frac{d\tilde{U}(t)}{dt} = -\mathbb{E} \left[r^* \left(\tilde{U}(t), \tilde{\mathbf{H}}(t) \right) \mid \tilde{U}(t) \right] (1 - \varepsilon) \quad (12)$$

where r^* is the DBP rate policy in (8) and the fictitious channel state is a white process⁷ with identical distribution as the actual CSIT $\hat{\mathbf{H}}$. Using the VCTS, the corresponding continuous time *average per-period unfinished work* $\overline{J^U}(\tilde{U}, t)$ and *average per-period energy consumption* $\overline{J^g}(\tilde{U}, t)$ are defined as follows:

$$\overline{J^U}(\tilde{U}, t) \triangleq \mathbb{E} \left[\int_t^T \tilde{U}(s) ds \mid \tilde{U}(t) \right] \quad (13)$$

$$\overline{J^g}(\tilde{U}, t) \triangleq \mathbb{E} \left[\int_t^T g \left(r^* \left(\tilde{U}(s), \tilde{\mathbf{H}}(s) \right), \tilde{\chi}(s) \right) ds \mid \tilde{U}(t) \right] \quad (14)$$

where $\tilde{\chi}(t) = (\tilde{U}(t), \tilde{\mathbf{H}}(t))$. ■

⁷It means that for any given t , the distribution of random variable $\tilde{\mathbf{H}}(t)$ is the same as that of the actual CSIT $\hat{\mathbf{H}}$. Furthermore, we have $\mathbb{E}[\tilde{\mathbf{H}}(t)] = \mathbb{E}[\hat{\mathbf{H}}] = \mathbf{0}$, $\mathbb{E}[\tilde{\mathbf{H}}(t_1)\tilde{\mathbf{H}}(t_2)] = \mathbb{E}[\hat{\mathbf{H}}\hat{\mathbf{H}}^H]\delta(t_1 - t_2)$.

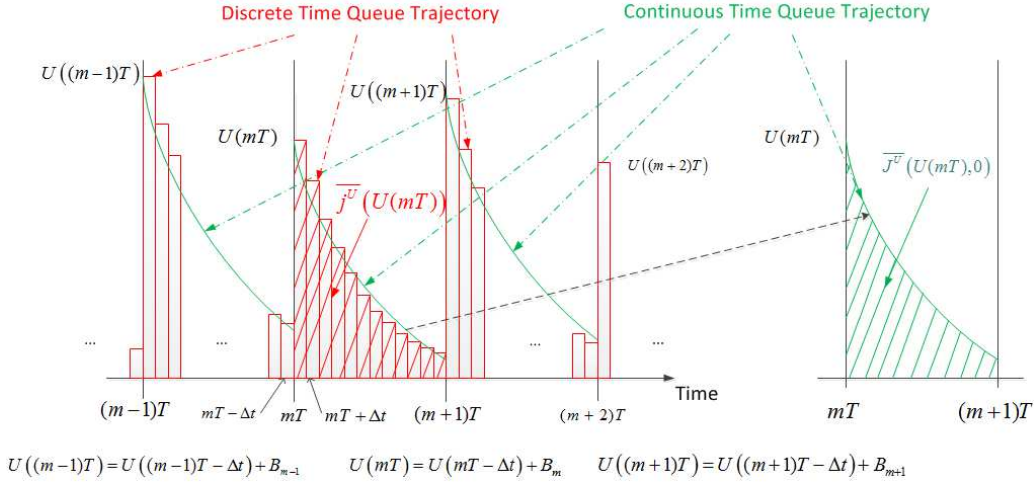


Fig. 3. Illustration of the discrete time and VCTS queue trajectory and the unfinished works $\{j^{\bar{U}}, \bar{J}^{\bar{U}}\}$ in one inter-arrival interval T .

Note that (13),(14) are the continuous-time counterparts of the discrete-time versions in ((10)),((11)). They measure the total queue length (total area) of the *queue trajectory* and total energy consumption (total area) of the *power trajectory* during an inter-arrival interval, respectively. The queue trajectory and $\{j^{\bar{U}}, \bar{J}^{\bar{U}}\}$ are illustrated in Fig. 3. To derive the actual per-period average unfinished work and energy consumption $\bar{j}^{\bar{U}}$ and \bar{j}^g in the discrete time, we first determine the continuous time counterparts using the following lemma.

Lemma 3 (Verification Lemma of $\bar{J}^{\bar{U}}$ and \bar{J}^g in VCTS): If there exists a continuous and differentiable function $\bar{J}^{\bar{U}*}(\tilde{U}, t)$ and $\bar{J}^g(\tilde{U}, t)$ satisfying the following partial differential equations (PDEs), respectively:

$$-\frac{\partial \bar{J}^{\bar{U}}}{\partial \tilde{U}}(1-\varepsilon)\mathbb{E}\left[r^*\left(\tilde{U}(t), \tilde{\mathbf{H}}(t)\right)\left|\tilde{U}(t)\right.\right] + \tilde{U}(t) + \frac{\partial \bar{J}^{\bar{U}}}{\partial t} = 0 \quad (15)$$

$$\mathbb{E}\left[g(r^*(\cdot), \tilde{\chi}(t))\left|\tilde{U}(t)\right.\right] - \frac{\partial \bar{J}^g}{\partial \tilde{U}}(1-\varepsilon)\mathbb{E}\left[r^*\left(\tilde{U}(t), \tilde{\mathbf{H}}(t)\right)\left|\tilde{U}(t)\right.\right] + \frac{\partial \bar{J}^g}{\partial t} = 0 \quad (16)$$

then, $\bar{J}^{\bar{U}*}(\tilde{U}, t)$ and $\bar{J}^g(\tilde{U}, t)$ are the total average unfinished work and total average energy consumption of the VCTS under the DBP in (12). \blacksquare

Proof: Note that (15),(16) resembles the Bellman equation of the discrete time dynamics in (10), (11). The proof is obtained using Taylor expansion of the value function and using the *divide-and-conquer* principle from (13),(14). Please refer to Appendix A for details. Using Lemma 3, the areas of the *queue trajectory* and the *power trajectory* can be obtained by solving the PDEs in (15),(16). \blacksquare

Finally, $\bar{j}^{\bar{U}}(U_0)$ and $\bar{j}^g(U_0)$ are related to the continuous time counterparts by the following Theorem.

Theorem 1 (Relationship between the Continuous Time and Discrete Time Unfinished Works): Let $\overline{J^{U^*}}(\tilde{U}, t)$ and $\overline{J^g}(\tilde{U}, t)$ be the solutions of the PDEs (15) and (16), respectively, in the virtual continuous time system. For sufficiently small Δt , the discrete-time per-period average unfinished work and energy consumption $\overline{j^U}$ and $\overline{j^g}$ are given by: $\overline{j^U}(U_0) = \overline{J^{U^*}}(U_0, 0) + \mathcal{O}(\Delta t)$ and $\overline{j^g}(U_0) = \overline{J^g}^*(U_0, 0) + \mathcal{O}(\Delta t)$. ■

Please refer to Appendix B for the proof. As a result of Theorem 1, we can focus on the continuous time equations to solve the area of queue and power trajectories and we can be assured that the solutions obtained will be accurate up to $\mathcal{O}(\Delta t)$. Using Lemma 3 and solving the associated PDEs in (15) and (16), we shall obtain an asymptotically accurate performance bounds of $\overline{J^{U^*}}(\tilde{U}, t)$ and $\overline{J^g}^*(\tilde{U}, t)$ which is summarized below.

Theorem 2 (Performance Bounds of $\overline{J^{U^}}(\tilde{U}, t)$ and $\overline{J^g}^*(\tilde{U}, t)$ in VCTS):* The per-period average unfinished work $\overline{J^{U^*}}(\tilde{U}, 0)$ in (13) and energy consumption $\overline{J^g}^*(\tilde{U}, 0)$ in (14) are given by

$$\overline{J^{U^*}}(\tilde{U}, 0) \leq \int_0^T y(t; \beta) dt \quad (17)$$

$$\overline{J^g}^*(\tilde{U}, 0) \geq \int_0^T \left[\frac{y(t; \beta') n_F (1 - \varepsilon)}{V} + \mathbb{E} \left[\left[\frac{\tilde{U}_0 n_F (1 - \varepsilon)}{V} - \frac{n_F}{f(\varepsilon, \sigma_e^2, \hat{\mathbf{H}})} \right]^+ + P_{cct} \right] - \frac{\tilde{U}_0 n_F (1 - \varepsilon)}{V} \right]^+ dt \quad (18)$$

where $y(t; \beta) = \exp \left[-\beta + \text{Ei}^{(-1)} \left[\text{Ei} \left(\log(\tilde{U}_0) + \beta \right) - n_F (1 - \varepsilon) e^{\beta t} \right] \right]$, $\beta = \mathbb{E} \left[\log((1 - \varepsilon) f(\varepsilon, \sigma_e^2, \hat{\mathbf{H}})) \right]$, and $\beta' = \mathbb{E} \left[\left(\log((1 - \varepsilon) f(\varepsilon, \sigma_e^2, \hat{\mathbf{H}})) \right)^+ \right]$. $\text{Ei}(x) = \int_{-\infty}^x e^t/t dt$ for $x > 0$, is the exponential integral function. The bounds are asymptotically accurate as V approaches 0. ■

Please refer to Appendix C for the proof.

B. Delay Analysis for Deterministic Arrivals

In this subsection, we establish the relationship between multiple per-period unfinished works and average end-to-end delay under the assumption of deterministic arrivals. Specifically, we assume the bit arrival \mathcal{B}_m is deterministic (given by B). The average bit arrival rate (bits per seconds) is given by $\overline{B} = B/T$. Such an arrival model embraces VoIP as well as other delay-sensitive source models derived from *constant bit rate* (CBR) encoders [28], [29]. Let $\bar{d}(\Omega^*)$ and $\bar{g}(\Omega^*)$ be the average end-to-end delay and the average power consumption, respectively, under DBP policy Ω^* in actual discrete time systems. $\bar{d}(\Omega^*)$ and $\bar{g}(\Omega^*)$ are

represented by the combination of per-period average unfinished work over multiple periods. We first have the following results regarding the steady state leftover bits of the buffer in VCTS due to the accumulated arrivals in the previous arrival periods.

Lemma 4 (Steady State Leftover Bits for the VCTS): Let L_m be the leftover bits of the buffer in VCTS at the end of the m -th arrival period. Given $L_0 < L^*$, then we have $\sup_{m \in \mathbb{R}^+} L_m \leq L^*$, and $L^* > 0$ satisfies the following fixed point equation:

$$L^* = e^{-\beta + \text{Ei}^{(-1)}[\text{Ei}(\log(B+L^*)+\beta) - (1-\varepsilon)n_F e^{\beta T}]} \quad (19)$$

Furthermore, the fixed point L^* exists and is unique. ■

Please refer to Appendix D for the proof. Based on Lemma 4, the average delay and power consumption for deterministic arrival is given by:

Theorem 3 (Average Delay and Average Power Consumption for Deterministic Arrivals): For sufficiently small Δt , the discrete-time average end-to-end delay $\bar{d}(\Omega^*)$ and average power consumption $\bar{g}(\Omega^*)$ under the DBP Ω^* with deterministic arrivals are given by:

$$\bar{d}(\Omega^*) \leq \frac{1}{B} \frac{1}{T} \overline{J^U}^*(B + L^*, 0) + \mathcal{O}(\Delta t) \quad (20)$$

$$\bar{g}(\Omega^*) \geq \frac{1}{T} \overline{J^g}^*(B, 0) + \mathcal{O}(\Delta t) \quad (21)$$

where B is the number of bits of an arrival packet in each period. ■

Proof: Please refer to Appendix E for the proof, where the relationship between the discrete model and the VCTS in Theorem 1 is utilized. ■

Corollary 1 (Asymptotic Power-Delay Tradeoff of DBP at Small Delay Regime): For sufficiently small V^8 , the asymptotic power-delay tradeoff of DBP of the VCTS is given by:

$$\bar{d}(\Omega^*) = \mathcal{O} \left(\frac{B^2}{\log(B\mathbb{E}[f(\epsilon, \sigma_e^2, \hat{\mathbf{H}})]/V)} + \frac{V}{\mathbb{E}[f(\epsilon, \sigma_e^2, \hat{\mathbf{H}})]} \right) \quad (22)$$

$$\bar{g}(\Omega^*) = \Omega \left(\left(\frac{B}{V} + P_{cct} \right) \frac{B}{\log(B\mathbb{E}[f(\epsilon, \sigma_e^2, \hat{\mathbf{H}})]/V)} \right) \quad (23)$$

⁸ V is a parameter that determines the tradeoff between power and delay in the system. For a given data arrival rate, small V corresponds to small delay regime.

Proof: Please refer to Appendix F for the proof. ■

Remark 3 (Interpretation of Results): Note that from Theorem 3, there is an additional $\mathcal{O}(\Delta t)$ term in (20) and (21) accounting for the approximation error between the power/delay of the original discrete time system and the VCTS. Yet, to simplify discussion, we focus on the first-order comparisons from the power-delay tradeoff of the VCTS in Corollary 1.

- **Comparison with CSIT-only policy:** The power-delay tradeoff result for the VCTS in Corollary 1 is asymptotically accurate as $V \rightarrow 0$ and this corresponds to small delay regime. For a given CSIT quality and P_{cct} , the conditional average data rate (conditioned on the queue state $\tilde{U}(t)$) for CSIT-only policy is given by:

$$\bar{r}_{CSIT} = E \left[r_{CSIT}(\tilde{\mathbf{H}}(t)|\tilde{U}(t)) \right] = \mathbb{E} \left[n_F \left\{ \log \left(\frac{(1-\varepsilon)f(\varepsilon, \sigma_e^2, \tilde{\mathbf{H}})}{V} \right) \right\}^+ \right]. \quad (24)$$

As a result, the power-delay tradeoff of the VCTS for CSIT-only policy [11] at small delay regime⁹ is given by $\bar{g} = \mathcal{O}(\exp(1/\bar{d}))$. On the other hand, since $\frac{1}{\log(1/V)} = \Omega(V)$, we have the delay and power of the VCTS given by $\bar{d}(\Omega^*) = \mathcal{O}\left(\frac{1}{\log(1/V)}\right)$, and $\bar{g}(\Omega^*) = \Omega\left(\frac{1}{V \log(1/V)}\right)$ from Corollary 1. Furthermore, since it is asymptotically accurate for small V (small delay regime), we can conclude that the power-delay tradeoff for DBP in the VCTS is given by $\bar{g} = \mathcal{O}(\bar{d} \exp(1/\bar{d}))$. Hence, compared with CSIT-only policy, the power consumption of DBP in the VCTS increases slower as delay \bar{d} tends¹⁰ to 0. Furthermore, we could achieve this superior tradeoff performance even with imperfect CSIT quality and non-ideal circuit power ($P_{cct} > 0$).

- **Effects of CSIT quality:** The penalty of CSIT quality is contained in $\mathbb{E}[f(\varepsilon, \sigma_e^2, \hat{\mathbf{H}})]$, which appears in the coefficients of the tradeoff equations in (22) and (23). For a given target PER ε , a larger CSIT error corresponds to a smaller $\mathbb{E}[f(\varepsilon, \sigma_e^2, \hat{\mathbf{H}})]$. Fig. 4 illustrates $\mathbb{E}[F_{\psi^2, s^2}^{-1}(\varepsilon)]$ versus CSIT errors σ_e^2 for target

⁹The delay expression for CSIT-only policy in [11] is derived using a discrete time approach and is given by $\bar{d} = \mathcal{O}\left(\frac{1}{\log(\bar{g})}\right) + 1$. On the other hand, the result in this paper is derived using a continuous time approach (VCTS) and the delay is given by $\bar{d} = \mathcal{O}\left(\frac{1}{\log(1/V)}\right) + \mathcal{O}(\Delta t)$ (for the actual discrete time system in terms of seconds). Hence, they match each other when expressing in terms of seconds.

¹⁰Note that while the delay of the VCTS can go to zero as $V \rightarrow 0$, the delay of the actual discrete time system cannot go to zero and is given by $\mathcal{O}(\Delta t)$ when $V \rightarrow 0$. This footnote applies to Corollary 2 as well.

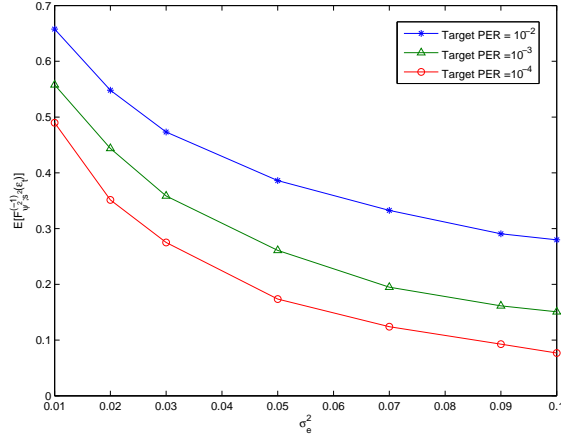


Fig. 4. Expectation of $F_{\psi^2, s^2}^{-1}(\epsilon)$ versus CSIT error σ_e^2 at different target PER.

PER 10^{-2} , 10^{-3} and 10^{-4} under the uniform power-delay profile.

- **Effects of P_{cct} :** From (23), the average power consumption has two components, namely the transmission power and the circuit power. The term $P_{cct}/(\log(Bf(\epsilon, \sigma_e^2, \hat{\mathbf{H}})/V))$ corresponds to the circuit power consumption, which increases with the burst transmission time in one arrival period. For small V , the burst transmission time decreases in the order of $\mathcal{O}(1/(\log(Bf(\epsilon, \sigma_e^2, \hat{\mathbf{H}})/V)))$. ■

C. Delay Analysis for Random Arrivals

In this subsection, we shall extend the analysis to i.i.d. random arrival process where the bit arrivals $\mathcal{B}_m \in [0, B_{max}]$ is generated by a general distribution $\Pr(\mathcal{B})$. The main results are summarized below.

Theorem 4 (Performance Bound of Average Delay and Power Consumption for Random Arrivals): For sufficiently small Δt , the discrete-time average end-to-end delay $\bar{d}_{iid}(\Omega^*)$ and average power consumption $\bar{g}_{iid}(\Omega^*)$ for DBP Ω^* under i.i.d. arrival process $\{\mathcal{B}_m\}$ are given by:

$$\bar{d}_{iid}(\Omega^*) \leq \frac{1}{\bar{B}_{iid}} \frac{1}{T} \mathbb{E}[\overline{J^U}^*(\mathcal{B} + L_{max}^*, 0)] + \mathcal{O}(\Delta t) \quad (25)$$

$$\bar{g}_{iid}(\Omega^*) \geq \frac{1}{T} \mathbb{E}[\overline{J^g}^*(\mathcal{B}, 0)] + \mathcal{O}(\Delta t) \quad (26)$$

where L_{max}^* is given by the fixed point of equation (19) (with $B = B_{max}$), \bar{B}_{iid} is the average bit arrival rate (bits per seconds) given by $\bar{B}_{iid} = \mathbb{E}[\mathcal{B}]/T$ and the expectation is taken w.r.t. the i.i.d. arrival process $\{\mathcal{B}_m\}$. ■

Proof: Please refer to Appendix G for the proof. ■

Corollary 2 (Asymptotic Power-Delay Tradeoff of DBP for Random Arrivals at Small Delay Regime): For sufficiently small V , the asymptotic power-delay tradeoff of DBP in the VCTS under random arrivals $\{\mathcal{B}_m\}$ is given by:

$$\bar{d}_{iid}(\Omega^*) = \mathcal{O} \left(\mathbb{E} \left[\frac{\mathcal{B}^2}{\log(\mathcal{B}\mathbb{E}[F_{\psi^2;s^2}^{-1}(\varepsilon)]/V)} \right] \right) \quad (27)$$

$$\bar{g}_{iid}(\Omega^*) = \Omega \left(\mathbb{E} \left[\left(\frac{\mathcal{B}}{V} + P_{cct} \right) \frac{\mathcal{B}}{\log(\mathcal{B}\mathbb{E}[F_{\psi^2;s^2}^{-1}(\varepsilon)]/V)} \right] \right) \quad (28)$$

Proof: The above results can be obtained in a similar way as Corollary 1 based on Theorem 4. ■

V. SIMULATION RESULTS AND DISCUSSIONS

In this section, we shall compare our proposed DBP with two reference baselines, namely the CSIT-only control policy (baseline 1) and No-CSIT policy (baseline 2). The baseline 1 policy allocates the rate and power to optimize the PHY throughput based on CSIT only. The baseline 2 policy always transmit with uniform power and fixed rate. In the simulation, we consider both deterministic and random arrivals. The OFDM systems has 1024 subcarriers with total bandwidth 10MHz. The scheduling slot duration Δt is 5msec. We simulate 10^6 scheduling slot to evaluate the average power and delay for different parameter V . The dashed lines that pass through the simulation point for DBP algorithm represents the analytical results in (22) and (23).

Fig. 5 illustrates the power-delay tradeoff at different CSIT errors $\sigma_e^2 = 0.01, 0.05, 0.1$. It can be observed that DBP simulation results match the performance bounds in Theorem 3 quite closely. In addition, it is obvious that DBP has significant gain compared with the CSIT-only policy and No-CSIT policy. It can be observed that the simulation points match with the analytical results very well for small V (which corresponds to small delay regime). As the CSIT error σ_e^2 gets smaller, the power-delay curve has steeper slope, which means better tradeoff. The performance gap between DBP and other policies increases at small delay and small CSIT error regime.

Fig. 7 shows that power-delay tradeoff with different circuit power consumption P_{cct} . It can be observed that the effect of P_{cct} is significant when P_{cct} is non-negligible from the total power consumption, especially

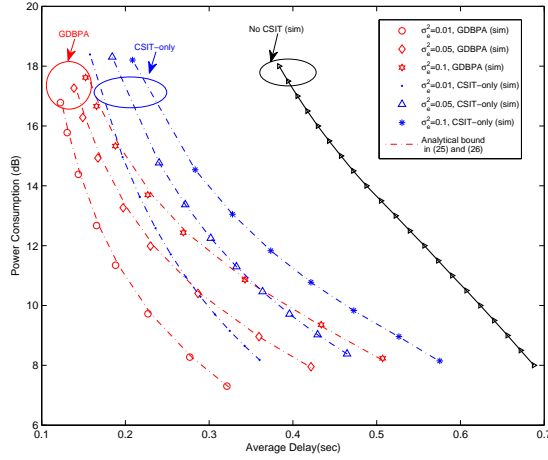


Fig. 5. Power-delay tradeoff for OFDM link at different CSIT errors for deterministic arrival. CSIT error variance ($\sigma_e^2 = 0.01, 0.05, 0.1$), traffic loading $\bar{B} = 1$ k nats/slot, $T=100$ msec, $\Delta t = 5$ msec, $P_{cct} = 0\%$, $n_F=1024$, $N_d=16$ and target PER =0.01. Note that V is a parameter that determines the tradeoff between power and delay. For example, $V = 1, 2, 4, 6, 10, 15, 25, 40$ at the marks along the DBP curves.

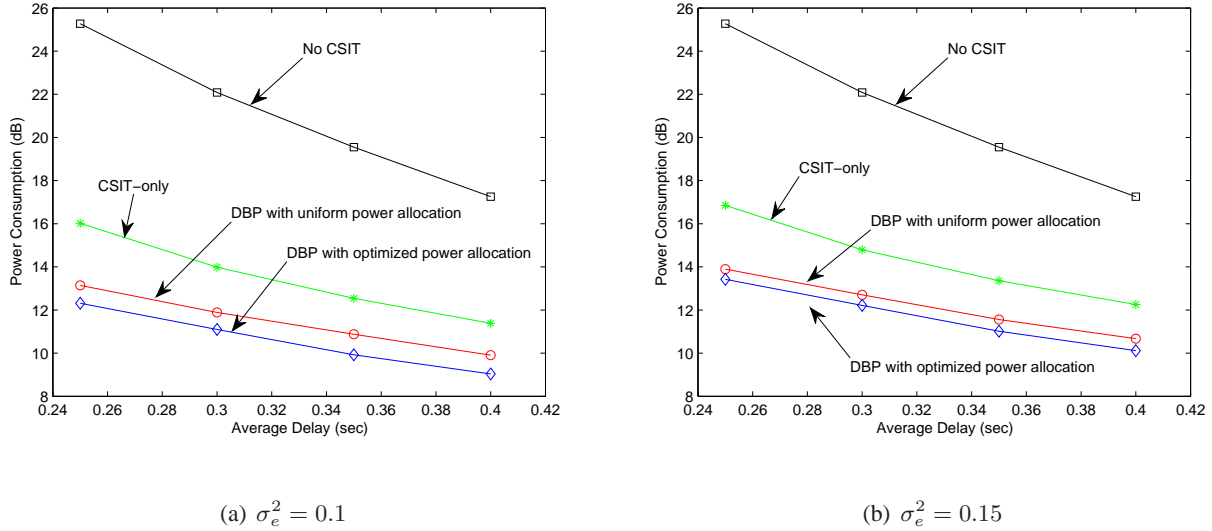


Fig. 6. Average Delay versus power consumption at different CSIT errors for deterministic arrival: traffic loading $\bar{B} = 1$ k nats/slot, $T=100$ msec, $\Delta t = 5$ msec, $P_{cct} = 0$, $n_F=1024$, $N_d = 16$, and target PER =0.01.

in the large delay regime. Similarly, the DBP has significant gain compared with the CSIT-only policy and No-CSIT policy.

Fig. 8 illustrates the power consumption versus CSIT errors at different delay requirements. It can be seen that when the CSIT error σ_e^2 increases, the minimum required power for satisfying the delay requirement

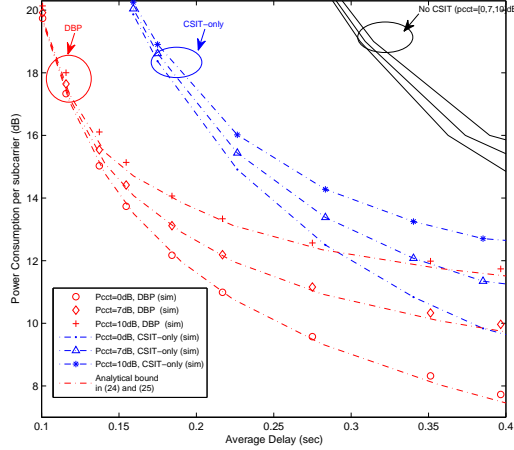


Fig. 7. Power-delay tradeoff for OFDM link at different P_{cct} for deterministic arrival. Traffic loading $\bar{B} = 0.8k$ nats/sec, $T=100$ msec, $\Delta t = 5$ msec, $P_{cct} = [0,7,10]$ dB, $\sigma_e^2 = 0.05$, $n_F=1024$, $N_d=16$ and target PER =0.01. Note that V is a parameter that determines the tradeoff between power and delay. For example, $V = 0.5, 1, 2, 4, 6, 10, 15, 25, 40$ at the marks along the DBP curves.

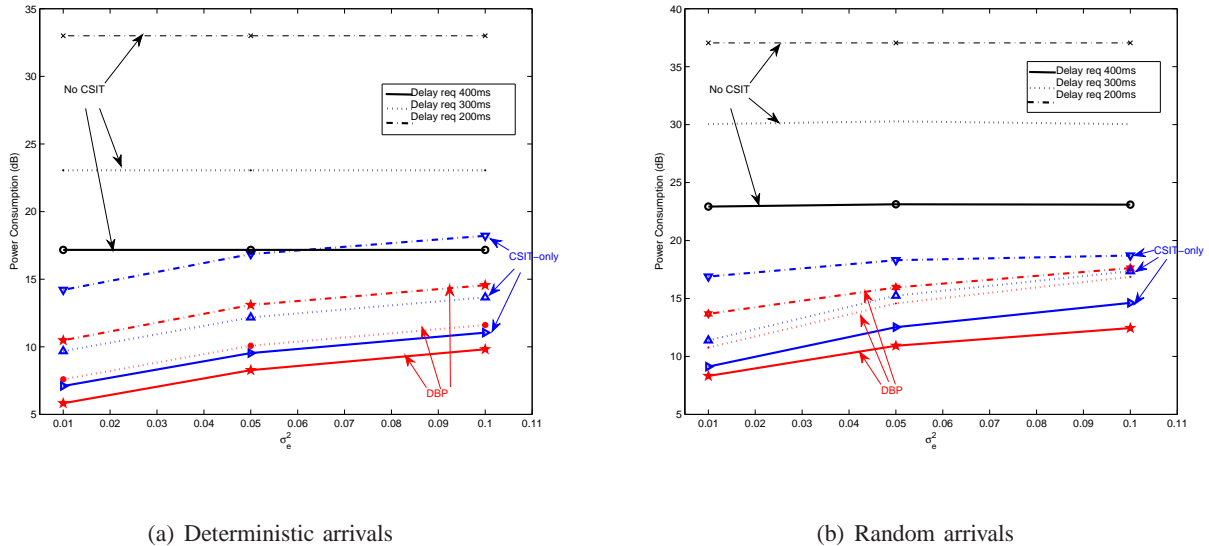


Fig. 8. Power consumption versus CSIT errors at different delay requirements: (a) Deterministic arrivals; (b) Random arrivals, traffic loading $\bar{B} = 10k$ nats/slot, $T=100$ msec, $\Delta t = 5$ msec, $P_{cct} = 10\%$, $n_F=1024$, $N_d = 16$, and target PER =0.01.

increases. In addition, the performance gain of the DBP decreases as the CSIT error increases.

VI. CONCLUSION

In this paper, we consider a tradeoff of power-delay in point-to-point OFDM systems with imperfect CSIT and non-ideal circuit power. Using Lyapunov optimization framework, we derive a dynamic backpressure

algorithm (DBP), which adapts the rate and power based on the instantaneous CSIT and QSI. To study how the CSIT quality and circuit power affects the power-delay tradeoff, we introduce a *virtual continuous time system* and derived an asymptotically accurate the power-delay bounds at small delay regime. We show that despite imperfect CSIT quality and non-ideal circuit power, the average power of the DBP policy scales with delay (D) as $\mathcal{O}(D \exp(1/D))$. The impact of CSIT quality and circuit power appears in the coefficients of the scaling law.

APPENDIX A: PROOF OF LEMMA 3

In order to obtain the continuous-time area under the queue trajectory in the VCTS, we shall use the principle of *divide-and-conquer* from the definition of $\overline{J^U}(\tilde{U}, t)$ in (13) and $\overline{J^g}(\tilde{U}, t)$ in (14). Specifically, we have

$$\overline{J^U}(\tilde{U}, t) = \mathbb{E} \left[\int_t^{t+t_\Delta} \tilde{U}(s) ds + \overline{J^U}(\tilde{U}, t+t_\Delta) \mid \tilde{U}(t) \right]$$

Using Taylor expansion $\overline{J^U}(\tilde{U}, t+t_\Delta) = \overline{J^U}(\tilde{U}, t) - \frac{\partial \overline{J^U}}{\partial \tilde{U}}(1-\varepsilon)r^*(\cdot)t_\Delta + \frac{\partial^2 \overline{J^U}}{\partial t^2}t_\Delta + \mathcal{O}(t_\Delta^2)$. For small value of t_Δ , $\tilde{U}(s)$ is assumed to be fixed to $\tilde{U}(t)$ for $s \in [t, t+t_\Delta]$. Thus, removing $\overline{J^U}(\tilde{U}, t)$ on both sides, we have

$$0 = \mathbb{E} \left[\tilde{U}(t)t_\Delta - \frac{\partial \overline{J^U}}{\partial \tilde{U}}(1-\varepsilon)r^*(\cdot)t_\Delta + \frac{\partial^2 \overline{J^U}}{\partial t^2}t_\Delta + \mathcal{O}(t_\Delta^2) \mid \tilde{U}(t) \right].$$

Dividing by t_Δ and taking the limit $t_\Delta \rightarrow 0$ gives (15). (16) is also obtained by a similar procedure from the definition of $\overline{J^g}(\tilde{U}, t)$ in (14).

APPENDIX B: PROOF OF THEOREM 1

Similar to Appendix A, using the principle of divide and conquer from the definition of $\overline{j^U}(U_0)$ in (10) and $\overline{j^g}(U_0)$ in (11), we shall have the following recursive equations in discrete-time systems:

$$\overline{j^U}(U_k) = \mathbb{E} \left[U_k \Delta t + \overline{j^U}(U_k - r^*(k)(1-\varepsilon)\Delta t) \mid U_k \right], \quad k = 0, \dots, \frac{T}{\Delta t} - 1 \quad (29)$$

$$\overline{j^g}(U_k) = \mathbb{E} \left[g(r(k), \chi(k)) \Delta t + \overline{j^g}(U_k - r^*(k)(1-\varepsilon)\Delta t) \mid U_k \right], \quad k = 0, \dots, \frac{T}{\Delta t} - 1 \quad (30)$$

where $r^*(k)$ is given by the DBP in (8). Since $\{\overline{j^U}, \overline{j^g}\}$ and $\{\overline{J^U}, \overline{J^g}\}$ satisfy the discrete time and continuous time recursive equations, respectively, we only need to show they are different in $\mathcal{O}(\Delta t)$.

We then discuss the property of $\overline{J^{U^*}}(\tilde{U}, t)$. Note that $\overline{J^{U^*}}(\tilde{U}, t)$ satisfies the PDE in (15), multiplying Δt in both sides of (15), we have:

$$\mathbb{E} \left[\tilde{U}(t)\Delta t + \frac{\partial \overline{J^U}}{\partial \tilde{U}} \{-r^*(\cdot)(1-\varepsilon)\} \Delta t + \frac{\partial \overline{J^U}}{\partial t} \Delta t \mid \tilde{U}(t) \right] = 0. \quad (31)$$

For simplicity, let $\overline{r^*} = \mathbb{E}[r^*(\tilde{U}(t), \tilde{\mathbf{H}}(t)) \mid \tilde{U}(t)]$. Since $\overline{r^*} = 0$ if $\tilde{U}(t) = 0$, by Taylor expansion on $\overline{J^U}(\tilde{U} - \overline{r^*}(1-\varepsilon)\Delta t, t + \Delta t)$, we have:

$$\overline{J^U}(\tilde{U} - \overline{r^*}(1-\varepsilon)\Delta t, t + \Delta t) - \overline{J^U}(\tilde{U}, t) = \frac{\partial \overline{J^U}}{\partial \tilde{U}}(-\overline{r^*}(1-\varepsilon))\Delta t + \frac{\partial \overline{J^U}}{\partial t}\Delta t + \mathcal{O}(\Delta t^2). \quad (32)$$

By substituting (32) into (31):

$$\overline{J^U}(\tilde{U}, t) = \mathbb{E} \left[\tilde{U}(t)\Delta t + \overline{J^U}(\tilde{U} - \overline{r^*}(1-\varepsilon)\Delta t, t + \Delta t) \mid \tilde{U}(t) \right] - \mathcal{O}(\Delta t^2). \quad (33)$$

Let $t = k\Delta t$, $\tilde{U}(k\Delta t) = \tilde{U}_k$ and $\overline{J^U}(\tilde{U}_k) = \overline{J^U}(\tilde{U}, k\Delta t)$, i.e., sampling at time $t = k\Delta t$,

$$\overline{J^U}(\tilde{U}_k) = \mathbb{E} \left[\tilde{U}_k\Delta t + \overline{J^U}_{k+1}(\tilde{U}_{k+1}) \mid \tilde{U}_k \right] - \mathcal{O}(\Delta t^2).$$

Compare to the discrete time recursive equation in (29), $\overline{J^U}(\tilde{U}_0, 0)$ satisfies it up to $\mathcal{O}(N\Delta t^2) = \mathcal{O}(\Delta t)$. As a result, the solution of continuous time PDE $\overline{J^U}^*(U_0, 0)$ will be different from the actual $\overline{j^U}(U_0)$ by at most $\mathcal{O}(\Delta t)$, i.e. $\overline{j^U}(U_0) = \overline{J^U}^*(U_0, 0) + \mathcal{O}(\Delta t)$. The case of the average energy consumption is obtained similarly.

APPENDIX C: PROOF OF THEOREM 2

In the proof, we shall first derive the bounds for the average departure rate and power consumption of the DBP policy, which is asymptotically tight at small delay regime (small V). Based on these bounds, we can derive the upper and lower bound of the queue trajectory and the corresponding bound of the average unfinished work and energy consumption.

First of all, we have the following lemma on the conditional average rate and power of the DBP policy.

Lemma 5 (Bounds on Conditional Average Policy): The conditional average rate and transmission power of DBP can be bounded by:

$$\overline{r}_{DBP}(\tilde{U}(t)) \triangleq \mathbb{E} \left[r_{DBP}(\chi) \mid \tilde{U}(t) \right] \in \left[\overline{r}_{low}(\tilde{U}(t)), \overline{r}_{up}(\tilde{U}(t)) \right] \quad (34)$$

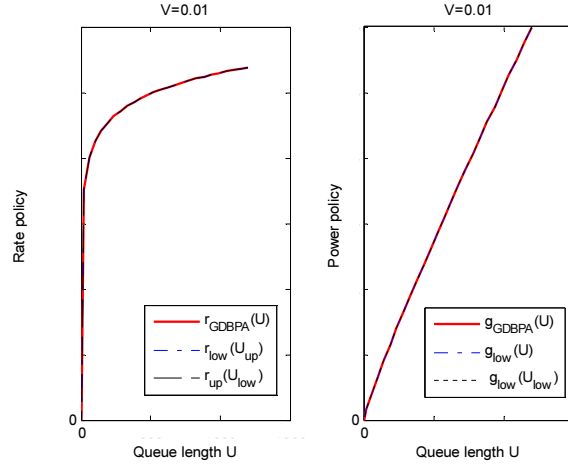


Fig. 9. Comparison of the actual and approximated rate and power control policies.

$$\bar{g}_{DBP}(\tilde{U}(t)) \triangleq \mathbb{E} \left[g_{DBP}(\chi) | \tilde{U}(t) \right] \geq \bar{g}_{low}(\tilde{U}(t)) \quad (35)$$

where

$$\bar{r}_{low}(\tilde{U}(t)) = \mathbb{E} \left[n_F \log \left\{ \frac{\tilde{U}(t)(1-\varepsilon)f(\varepsilon, \sigma_e^2, \hat{\mathbf{H}})}{V} \right\} | \tilde{U}(t) \right]^+ = \left[n_F \log(\tilde{U}(t)) + n_F \beta \right]^+,$$

$$\bar{r}_{up}(\tilde{U}(t)) = n_F \mathbb{E} \left[\left(\log \tilde{U}(t) \right)^+ + \left(\log \frac{(1-\varepsilon)f(\varepsilon, \sigma_e^2, \hat{\mathbf{H}})}{V} \right)^+ | \tilde{U}(t) \right] = n_F \left[\log(\tilde{U}(t)) \right]^+ + n_F \beta', \quad (36)$$

$$\text{and } \bar{g}_{low}(\tilde{U}(t)) = \left[\frac{\tilde{U}(t)(1-\varepsilon)n_F}{V} + \bar{g}_{DBP}(\tilde{U}(t_0)) - \frac{\tilde{U}(t_0)(1-\varepsilon)n_F}{V} \right]^+. \quad \blacksquare$$

As a result, we can approximate \bar{r}_{DBP} and \bar{g}_{DBP} using $\bar{r}_{low}(U)$ and $\bar{g}_{low}(U)$ with asymptotically small approximation errors at small V . Fig. 9 illustrates the accuracy of the approximation.

Proof: The key proof is to find the bound for the average departure rate. Specifically, from (8), using Jensen's inequality yields following inequality, we have the lower bound:

$$\bar{r}_{DBP}(\tilde{U}(t)) = \mathbb{E} \left[\left(n_F \log \left\{ \frac{\tilde{U}(t)(1-\varepsilon)f(\varepsilon, \sigma_e^2, \hat{\mathbf{H}})}{V} \right\} \right)^+ | \tilde{U}(t) \right] \geq \bar{r}_{low}(\tilde{U}(t)). \quad (37)$$

Similarly, using the fact that $(x+y)^+ \leq (x^+ + y^+)$, we have the upper bound:

$$\bar{r}_{DBP}(\tilde{U}(t)) = n_F \mathbb{E} \left[\left(\log \left\{ \tilde{U}(t) \right\} + \log \left\{ \frac{(1-\varepsilon)f(\varepsilon, \sigma_e^2, \hat{\mathbf{H}})}{V} \right\} \right)^+ | \tilde{U}(t) \right] \leq \bar{r}_{up}(\tilde{U}(t)).$$

Now, we shall show the lower bound of $\bar{g}_{DBP}(\tilde{U}(t))$. Let $f(\varepsilon, \sigma_e^2, \hat{\mathbf{H}}) = X$ and $q(x)$ to be the pdf of the random variable X , where the randomness is induced by the CSIT $\hat{\mathbf{H}}$. From (9), we have:

$$\bar{g}_{DBP}(\tilde{U}(t)) = \mathbb{E} \left[\left(\frac{\tilde{U}(t)n_F(1-\varepsilon)}{V} - \frac{n_F}{X} \right)^+ + P_{cct} | \tilde{U}(t) \right] = \int_{\frac{V}{\tilde{U}(1-\varepsilon)}}^{\infty} \left(\frac{\tilde{U}n_F(1-\varepsilon)}{V} - \frac{n_F}{X} + P_{cct} \right) q(x) dx.$$

$\bar{g}_{DBP}(\tilde{U}(t))$ is a monotonic increasing function of $\tilde{U}(t)$. Differentiating both sides w.r.t. \tilde{U} :

$$\frac{d\bar{g}_{DBP}(\tilde{U})}{d\tilde{U}} = \frac{(1-\varepsilon)n_F}{V} \int_{\frac{V}{\tilde{U}(1-\varepsilon)}}^{\infty} q(x) dx \leq \frac{(1-\varepsilon)n_F}{V}, \quad \forall \bar{g}_{DBP}(\tilde{U}) \geq 0.$$

As a result, we can construct a lower bound of \bar{g}_{DBP} by the following ODE:

$$\frac{d\bar{g}_{low}(\tilde{U})}{d\tilde{U}} = \begin{cases} \frac{(1-\varepsilon)n_F}{V}, & \text{if } \tilde{U} \in \Theta_1 \\ 0 & , \text{ otherwise} \end{cases} \quad (38)$$

$$\bar{g}_{low}(\tilde{U}_0) = \bar{g}_{DBP}(\tilde{U}_0) \quad (39)$$

where Θ_1 is $\{\tilde{U} \mid \bar{g}_{low}(\tilde{U}) \geq 0\}$. $\bar{g}_{low}(\tilde{U})$ always has steeper slope compared with $\bar{g}_{DBP}(\tilde{U})$ and together with the monotonic increasing property of $\bar{g}_{DBP}(\tilde{U})$, we could establish the lower bound by solving (38) and (39). ■

Secondly, based on Lemma 5, we shall derive an upper bound on $\overline{J^{U^*}}(\tilde{U}, t)$ by solving the PDE in Lemma

3. Specifically, the queue dynamics $\tilde{U}(t)$ satisfies the ODE in the VCTS in (12):

$$\frac{d\tilde{U}}{dt} = -\bar{r}_{DBP}(\tilde{U})(1-\varepsilon) \leq -\bar{r}_{low}(\tilde{U})(1-\varepsilon). \quad (40)$$

Hence, the upper bound queue trajectory is given by:

$$\tilde{U}(t) \leq \tilde{U}_{up}(t) = \exp\left[-\beta + \text{Ei}^{(-1)}\left[\text{Ei}\left(\log(\tilde{U}_0) + \beta\right) - (1-\varepsilon)n_F e^{\beta t}\right]\right] = y(t; \beta), \quad (41)$$

Based on (13), we have

$$\overline{J^{U^*}}(\tilde{U}, 0) \approx \mathbb{E}\left[\int_0^T \tilde{U}(t) dt \mid \tilde{U}_0\right] \leq \int_0^T \tilde{U}_{up}(t) dt$$

which yields the upper bound of $\overline{J^{U^*}}(\tilde{U}, 0)$ in (17).

Finally, we shall derive a lower bound for $\overline{J^g}(\tilde{U}, 0)$. Using $\bar{r}_{up}(\tilde{U}(t))$, we can construct a lower bound trajectory by solving $\frac{d\tilde{U}_{low}}{dt} = -\bar{r}_{up}(\tilde{U}_{low})(1-\varepsilon)$, and the solution is given by:

$$\tilde{U}(t) \geq \tilde{U}_{low}(t) = \exp\left[-\beta' + \text{Ei}^{(-1)}\left[\text{Ei}\left(\log(\tilde{U}_0) + \beta'\right) - (1-\varepsilon)n_F e^{\beta' t}\right]\right] = y(t; \beta'), \quad (42)$$

At any time $t \in [0, T]$, we have

$$\bar{g}_{low}(\tilde{U}_{low}(t)) \leq \bar{g}_{low}(\tilde{U}(t)) \leq \bar{g}_{DBP}(\tilde{U}(t)). \quad (43)$$

Hence,

$$\overline{Jg^*}(\tilde{U}, 0) = \int_0^T \overline{g}_{DBP}(\tilde{U}(t)) dt \geq \int_0^T \left[\frac{\tilde{U}_{low}(t)n_F(1-\varepsilon)}{V} + \overline{g}_{DBP}(\tilde{U}_0) - \frac{\tilde{U}_0 n_F(1-\varepsilon)}{V} \right]^+ dt$$

which yields the lower bound of per-period average energy consumption in (18).

APPENDIX D: PROOF OF LEMMA 4

Using the theory developed for the continuous time model in Section IV-A, it is enough to show that L_m for the VCTS is bounded by L^* for all m . First of all, we shall show that L^* is unique.

Specifically, the leftover bits at the end of the m -th period L_m is:

$$\underline{l}_m \leq L_m \leq \overline{l}_m \quad (44)$$

where \overline{l}_m and \underline{l}_m are the leftover bits of m -th period of approximated queue trajectory $\tilde{U}_{up}(t)$ and $\tilde{U}_{low}(t)$ in (41) and (42), respectively. Recall that $\tilde{U}_{low}(t) \leq \tilde{U}(t) \leq \tilde{U}_{up}(t)$. Since the unfinished work at the start epoch of m -th period is the summation of arriving bits B and the leftover bits of the previous $(m-1)$ -th period, \overline{l}_m and \underline{l}_m satisfy the followings:

$$\overline{l}_m = \overline{f}(B + \overline{l}_{m-1}) \quad \text{and} \quad \underline{l}_m = \underline{f}(B + \underline{l}_{m-1})$$

where $\overline{f}(x) = \exp[-\beta + \text{Ei}^{(-1)}[\text{Ei}(\log(x) + \beta) - n_F(1-\varepsilon)e^{\beta T}]]$, and $\underline{f}(x) = \exp[-\beta' + \text{Ei}^{(-1)}[\text{Ei}(\log(x) + \beta') - n_F(1-\varepsilon)e^{\beta' T}]]$. Both $\overline{f}(x)$ and $\underline{f}(x)$ are the increasing functions of x since the exponential integral Ei is increasing function. Note that the slope of $\overline{f}(x)$ is given by:

$$\frac{d\overline{f}(x)}{dx} = \frac{\text{Ei}^{(-1)}[\text{Ei}(\log(x) + \beta) - (1-\varepsilon)n_F e^{\beta T}]}{\log(x) + \beta} < 1, \quad \text{for all } x > 0.$$

Therefore, there exists a unique crossing point between $y = x$ and $y = \overline{f}(B+x)$ and this proved the existence and uniqueness of L^* .

Finally, we shall try to prove that $\sup_{m \in \mathbb{R}^+} L_m$ is bounded by L^* . We first claim that $\overline{l}_m \leq L^*$ for all m . From (19) and $\overline{l}_m = \overline{f}(B + \overline{l}_{m-1})$, we have:

$$\text{Ei}(\log(L^*) + \beta) = \text{Ei}(\log(B + L^*) + \beta) - (1-\varepsilon)n_F e^{\beta T} \quad (45)$$

$$\text{Ei}(\log(\overline{l}_m) + \beta) = \text{Ei}(\log(B + \overline{l}_{m-1}) + \beta) - (1-\varepsilon)n_F e^{\beta T} \quad (46)$$

Subtracting (46) from (45), we have

$$\int_{\log(\bar{l}_m)+\beta}^{\log(L^*)+\beta} \frac{e^x}{x} dx = \int_{\log(B+\bar{l}_{m-1})+\beta}^{\log(B+L^*)+\beta} \frac{e^x}{x} dx. \quad (47)$$

Note that e^x/x is positive for $x > 0$, and $\log(\bar{l}_m) + \beta > 0$ due to $\bar{f}(x) > e^{-\beta}$. If $\{\bar{l}_m\}$ is not bounded by L^* , there exists m' such that $\bar{l}_{m'-1} \leq L^* < \bar{l}_{m'}$ and $B + \bar{l}_{m'-1} \leq B + L^* < B + \bar{l}_{m'}$. This m' makes the RHS of (47) positive while the LHS of (47) becomes negative which means a contradiction. Thus, $\{\bar{l}_m\}$ is bounded by L^* . As a result, $\sup_{m \in \mathbb{R}^+} L_m$ is bounded by L^* .

APPENDIX E: PROOF OF THEOREM 3

In the proof, we shall use Little's law [30] to derive the average delay and power consumption for the real discrete time system.

Specifically, under the stationary DBP policy, the system state $\chi(k)$ evolves as an ergodic Markov chain and hence, there exists a steady state distribution π_χ such as $\pi_\chi(\chi_0) = \lim_{k \rightarrow \infty} \Pr[\chi(k) = \chi_0]$. Using Little's law and the characteristic of ergodic chain, the average end-to-end delay under the stationary DBP policy Ω^* is given by:

$$\bar{d}(\Omega^*) = \frac{1}{B} E_{\pi_\chi}[U(k)] = \frac{1}{B} \lim_{K \rightarrow \infty} \sum_{k=0}^{K-1} \frac{1}{K} \mathbb{E}[U(k) | U(0)]$$

where the E_{π_χ} is the expectation w.r.t. the steady state distribution of $U(k)$. Using ergodic theory, we have:

$$\bar{d}(\Omega^*) = \frac{1}{BT} \lim_{M \rightarrow \infty} \frac{1}{M} \sum_{m=0}^{M-1} \bar{j}^{U^*}(U_0^m)$$

where U_0^m is the initial queue length of the m -th period. Note that the unit of $\bar{B}T$ is bits, and the unit of \bar{j}^{U^*} is bits \times seconds, and hence the unit of \bar{d} is seconds. As shown in Lemma 4, the leftover L_m at the end of the m -th arrival period is bounded by L^* . Hence, U_0^m is upper bounded by $B + L^*$. Using the relationship between the unfinished works in discrete time and continues time in Theorem 1, the discrete time average delay given by:

$$\bar{d}(\Omega^*) \leq \frac{1}{BT} \bar{j}^{U^*}(B + L^*) = \frac{1}{BT} \bar{J}^{U^*}(B + L^*, 0) + \mathcal{O}(\Delta t).$$

Similarly, the average power consumption $\bar{g}(\Omega^*)$ is given by:

$$\bar{g}(\Omega^*) = \frac{1}{T} \lim_{M \rightarrow \infty} \frac{1}{M} \sum_{m=0}^{M-1} \bar{j}^{g^*}(U_0^m) \geq \frac{1}{T} \bar{j}^{g^*}(B) = \frac{1}{T} \bar{J}^{g^*}(B, 0) + \mathcal{O}(\Delta t).$$

Note that the unit of T is seconds, and the unit of $\overline{jg^*}$ is Watt \times seconds, and hence the unit of \overline{g} is Watt.

APPENDIX F: PROOF OF COROLLARY 1

From the Theorem 3, we only need to obtain $\overline{jU^*}(B + L^*)$ and $\overline{jg^*}(B, 0)$ for the continuous time model by studying the continuous queue trajectory.

First of all, we show the asymptotic behavior of L^* as V goes to 0. Let x to be β for simplifying notation. From (19), we have: $L^* = e^{-x + \text{Ei}^{(-1)}[\text{Ei}(\log(B + L^*) + x) - n_F(1 - \varepsilon)e^x]}$. As V goes to 0, β and x increase since $\beta = \Theta(\log(1/V))$. For $x > 0$, e^x increases faster than $\text{Ei}(x)$ because

$$\text{Ei}(x) = \log x + \gamma + \sum_{k=1}^{\infty} \frac{x^k}{k k!} < \sum_{k=1}^{\infty} \frac{x^k}{k!} = e^x.$$

Hence, as V approaches to 0, we have $L^* = \Theta(e^{-\beta}) = \Theta\left(\frac{V}{\mathbb{E}[f(\varepsilon, \sigma_e^2, \hat{\mathbf{H}})]}\right)$

Secondly, we shall obtain the asymptotic area of buffer trajectory. Specifically, we use Fig. 10 to illustrate the proof. The upper bound of queue delay can be derived from the area of $\tilde{U}_{up}(t)$ in (41). As shown in (40), $d\tilde{U}_{up}/dt \propto \log \tilde{U}_{up}(t)$, which is decreasing in t . Hence, $\tilde{U}_{up}(t)$ is a convex function in t and we could upper bound $\overline{jU^*}(B + L^*, 0)$ by the summation of the triangle area (A) and the rectangle area (B) as illustrated in Fig. 10(a):

$$\overline{jU^*}(B + L^*, 0) \leq \frac{1}{2}(B - L_{\Delta})t_d + T(L^* + L_{\Delta}). \quad (48)$$

where $L_{\Delta} = \Theta(e^{-\beta})$ and t_d is the time when $\tilde{U}_{up}(t) = L^* + L_{\Delta}$ which is given by:

$$t_d = \frac{e^{-\beta}}{(1 - \varepsilon)n_F} \{\text{Ei}(\log(B + L^*) + \beta) - \text{Ei}(\log(L^* + L_{\Delta}) + \beta)\} = \Theta\left(\frac{B}{\log(B\mathbb{E}[f(\varepsilon, \sigma_e^2, \hat{\mathbf{H}})]/V)}\right)$$

From (48), the upper bound of average delay $\overline{d}(\Omega^*)$ is given by (22).

Then, we focus on deriving $\overline{jg^*}(B, 0)$. Specifically, we use Fig. 10 to illustrate the proof. We elaborate the asymptotic expression using $\overline{g}_{low}(\tilde{U}_{low}(t))$ where $\tilde{U}_{low}(t)$ is the lower bound trajectory derived using \overline{r}_{up} in (42). According to (43), \overline{g}_{low} is a lower bound of the actual power trajectory and it is a convex function of t . As a result, the lower bound of the transmission energy (area of \overline{g}_{low}) is given by the triangle (C) of the tangent line of the $\overline{g}_{low}(B)$ as illustrated in Fig. 10(b). Let t_p to be the time when the tangent line touches

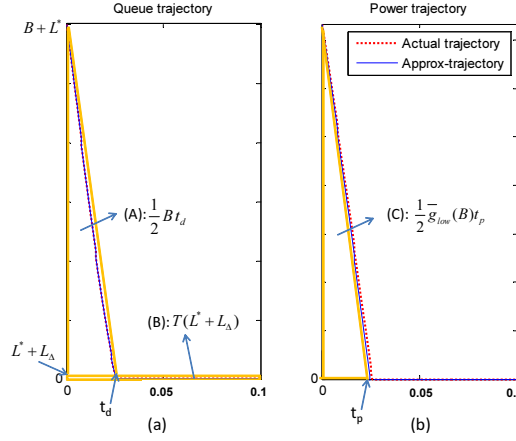


Fig. 10. Asymptotic upper bound of the area below the queue and power trajectory.

zero which is given by

$$t_p = \frac{\bar{g}_{low}(B)}{-\left.\frac{d\bar{g}_{low}(\tilde{U}(t))}{dt}\right|_{\tilde{U}=B}} = \frac{\mathbb{E}\left[\left[\frac{Bn_F(1-\varepsilon)}{V} - \frac{n_F}{f(\varepsilon, \sigma_e^2, \hat{\mathbf{H}})}\right]^+ + P_{cct}\right]}{\frac{1}{V}\bar{r}^*(\tilde{U})\Big|_{\tilde{U}=B}} = \Theta\left(\frac{B}{\log(B\mathbb{E}[f(\varepsilon, \sigma_e^2, \hat{\mathbf{H}})]/V)}\right).$$

Note that t_p means the transmission time for the burst transmission. On the other hand, we get the same order of t_p in the case of that \bar{g}_{low} is a concave function¹¹. Hence, the asymptotic lower bound for the total energy consumption in one period is given by:

$$\bar{J}^g(B, 0) \geq \frac{1}{2}\bar{g}_{low}(B)t_p \approx \mathbb{E}\left[\left(\frac{Bn_F(1-\varepsilon)}{V} - \frac{n_F}{f(\varepsilon, \sigma_e^2, \hat{\mathbf{H}})^+}\right)\right]t_p + P_{cct}t_p$$

which yields the lower bound of average power consumption in (23).

APPENDIX G: PROOF OF THEOREM 4

To derive the bound for the random bits arrival, we shall first derive the upper bound of the steady state leftover queue length of a period (where the lower bound is 0 obviously.)

First of all, from the results of deterministic arrivals in Theorem 3, the average end-to-end delay $\tilde{d}(\Omega^*)$ and the average power consumption $\tilde{g}(\Omega^*)$ for random arrivals are given by:

$$\begin{aligned}\tilde{d}(\Omega^*) &= \frac{1}{BT}\mathbb{E}\left[\bar{J}^U(B + \mathcal{L}, 0)\right] + \mathcal{O}(\Delta t) \\ \tilde{g}(\Omega^*) &= \frac{1}{T}\mathbb{E}\left[\bar{J}^g(B + \mathcal{L}, 0)\right] + \mathcal{O}(\Delta t)\end{aligned}$$

¹¹The t_p of the concave case is obtained from $\bar{g}_{low}(\tilde{U}_{low}(t_p)) = 0$.

where \mathcal{L} is the steady state leftover queue length of a period for random arrivals. From Lemma 4, it is obvious that L_{max}^* is the upper bound of \mathcal{L} . Then we have the upper bound and lower bound of average per-period unfinished work and energy consumption in VCTS: $\mathbb{E} \left[\overline{JU}^*(\mathcal{B} + \mathcal{L}, 0) \right] \leq \mathbb{E} \left[\overline{JU}^*(\mathcal{B} + L_{max}^*, 0) \right]$ and $\mathbb{E} \left[\overline{Jg}^*(\mathcal{B} + \mathcal{L}, 0) \right] \geq \mathbb{E} \left[\overline{Jg}^*(\mathcal{B}, 0) \right]$, which yield (25) and (26), respectively.

REFERENCES

- [1] F. Meshkati, H.V. Poor, and S.C. Schwartz. Energy-Efficient resource allocation in wireless networks. *IEEE Signal Processing Magazine*, 24(3):58–68, 2007.
- [2] Mingbo Xiao, N.B. Shroff, and E.K.P. Chong. A utility-based power-control scheme in wireless cellular systems. *IEEE/ACM Transactions on Networking*, 11(2):210–221, 2003.
- [3] F. Rey, M. Lamarca, and G. Vazquez. Robust power allocation algorithms for MIMO OFDM systems with imperfect CSI. *IEEE Transactions on Signal Processing*, 53(3):1070–1085, 2005.
- [4] Yingwei Yao and G.B. Giannakis. Rate-maximizing power allocation in OFDM based on partial channel knowledge. *IEEE Transactions on Wireless Communications*, 4(3):1073–1083, 2005.
- [5] T. Yoo and A. Goldsmith. Capacity and power allocation for fading MIMO channels with channel estimation error. *IEEE Transactions on Information Theory*, 52(5):2203–2214, 2006.
- [6] D.J. Love, R.W. Heath, V.K.N. Lau, D. Gesbert, B.D. Rao, and M. Andrews. An overview of limited feedback in wireless communication systems. *IEEE Journal on Selected Areas in Communications*, 26(8):1341–1365, 2008.
- [7] D. P Bertsekas. *Dynamic programming: deterministic and stochastic models*. Prentice-Hall, Inc. Upper Saddle River, NJ, USA, 1987.
- [8] L. Tassiulas and A. Ephremides. Stability properties of constrained queueing systems and scheduling policies for maximum throughput in multihop radio networks. *IEEE Transactions on Automatic Control*, 37(12):1936–1948, 1992.
- [9] L. Georgiadis, M. J Neely, and L. Tassiulas. *Resource allocation and cross layer control in wireless networks*. Now Pub, 2006.
- [10] M. J. Neely. Energy optimal control for time-varying wireless networks. *IEEE Transactions on Information Theory*, 52(7):2915–2934, 2006.
- [11] Randall Berry. Optimal power-delay trade-offs in fading channels: Small delay asymptotics. *Information Theory and Applications Inaugural Workshop*, 2006.
- [12] Daji Qiao, Sunghyun Choi, Amit Jain, and Kang G Shin. MiSer: an optimal low-energy transmission strategy for IEEE 802.11a/h. In *Proceedings of the 9th annual international conference on Mobile computing and networking*, MobiCom '03, page 161175, New York, NY, USA, 2003. ACM. ACM ID: 939003.
- [13] M. Zafer and E. Modiano. Minimum energy transmission over a wireless channel with deadline and power constraints. *IEEE Transactions on Automatic Control*, 54(12):2841–2852, 2009.

- [14] Harold Joseph Kushner and Paul Dupuis. *Numerical methods for stochastic control problems in continuous time*. Springer, 2001.
- [15] D.P. Bertsekas. *Dynamic programming and optimal control*. Athena Scientific, 2007.
- [16] M. A Zafer and E. Modiano. A calculus approach to minimum energy transmission policies with quality of service guarantees. In *IEEE INFOCOM*, volume 1, page 548, 2005.
- [17] T.L. Marzetta and B.M. Hochwald. Fast transfer of channel state information in wireless systems. *IEEE Transactions on Signal Processing*, 54(4):1268–1278, 2006.
- [18] T. Yoo and A. Goldsmith. Capacity and power allocation for fading MIMO channels with channel estimation error. *IEEE Transactions on Information Theory*, 52(5):2203–2214, 2006.
- [19] T. R. Ramya and S. Bhashyam. Eigen-Beamforming with Delayed Feedback and Channel Prediction. In *Proc. ISIT*, June-July 2009.
- [20] D. P. Bertsekas and J. N. Tsitsiklis. *Neuro-Dynamic Programming*. Athena Scientifics, 1st edition, 1996.
- [21] V. S. Borkar. *Stochastic Approximation: A Dynamical Systems Viewpoints*. Cambridge University Press, United Kingdom, 1st edition, 2008.
- [22] V. Lau, Wing Kwan Ng, and D.S.W. Hui. Asymptotic tradeoff between cross-layer goodput gain and outage diversity in OFDMA systems with slow fading and delayed CSIT. *IEEE Transactions on Wireless Communications*, 7(7):2732–2739, 2008.
- [23] IEEE 802.16m evaluation methodology document. IEEE 802.16m-08/004r4.
- [24] J. G. Proakis. *Digital Communications*. New York: McGraw-Hill, 4th ed., 2001.
- [25] R. A. Berry and R. G. Gallager. Communication over fading channels with delay constraints. *IEEE Transactions on Information Theory*, 48(5):1135–1149, 2002.
- [26] Shuguang Cui, A.J. Goldsmith, and A. Bahai. Energy-constrained modulation optimization. *IEEE Transactions on Wireless Communications*, 4(5):2349–2360, 2005.
- [27] M. Andrews, K. Kumaran, K. Ramanan, A. Stolyar, R. Vijayakumar, and P. Whiting. Scheduling in a queuing system with asynchronously varying service rates. *Probability in the Engineering and Informational Sciences*, 18(02):191–217, 2004.
- [28] Eunkyung Kim, Juhee Kim, and Kyung Soo Kim. An efficient resource allocation for TCP services in IEEE 802.16 wireless MANs. In *Vehicular Technology Conference, 2007. VTC-2007 Fall. 2007 IEEE 66th*, pages 1513–1517, 2007.
- [29] Mirosław Narbutt and Mark Davis. Gauging VoIP call quality from 802.11 WLAN resource usage. In *A World of Wireless, Mobile and Multimedia Networks, International Symposium on*, volume 0, pages 315–324, Los Alamitos, CA, USA, 2006. IEEE Computer Society.
- [30] S. M. Ross. *Introduction to probability models*. 8th edition, Amsterdam : Academic Press, 2003.